Analytical Methods

Accepted Manuscript

This article can be cited before page numbers have been issued, to do this please use: J. Look, S. R. Ahmed, M. H. Mahana, M. Shalauddin, S. Akhter, W. J. Basirun, S. Srinivasan and A. R. Rajabzadeh, *Anal. Methods*, 2026, DOI: 10.1039/D6AY00361C.

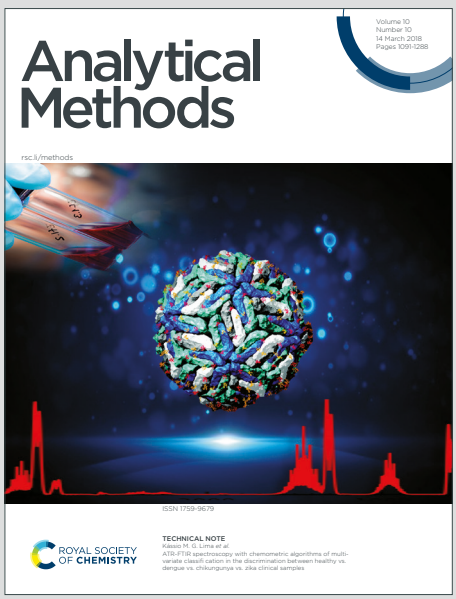

ROYAL SOCIETY OF CHEMISTRY

rsc.li/methods

View Article Online
DOI: 10.1039/D6AY00361C

Electrochemically Amplified Nanozymatic Activity of Biolinker-based Synthesized Co-MOF for H_2O_2 and Dopamine Detection

Jasmine Look[1], Syed Rahin Ahmed*[1], Mohamed Hassan Mahana[2,3], Md. Shalauddin*[4], Shamima Akhter*[5], Wan Jefrey Basirun[6,7*], Seshasai Srinivasan*[1,2] and Amin Reza Rajabzadeh*[1,2]

[1]W Booth School of Engineering Practice and Technology, McMaster University, 1280 Main Street West Hamilton, Ontario, Canada L8S 4L7
[2]School of Biomedical Engineering, McMaster University, 1280 Main Street West Hamilton, Ontario, Canada L8S 4L7
[3]Department of Pharmaceutical Analytical Chemistry, Faculty of Pharmacy, Tanta University, Tanta 3111, Egypt
[4]School of Pharmacy, Faculty of Health and Medical Sciences, Taylor's University, Subang Jaya, Selangor 47500, Malaysia
[5]Department of Pharmaceutical Chemistry, School of Pharmacy, IMU University, Bukit Jalil, 57000 Kuala Lumpur, Malaysia.

[6]Nanotechnology and Catalysis Research Center (NANOCAT), Universiti Malaya, 50603 Kuala Lumpur, Malaysia.
[7]Department of Chemistry, Faculty of Science, Universiti Malaya, 50603 Kuala Lumpur, Malaysia.

E-mail address: SRA: ahmes91@mcmaster.ca, MS: md.shalauddin@taylors.edu.my , SA: shamimaakhter@imu.edu.my, WJB: jeff@um.edu.my, SS:ssriniv@mcmaster.ca, ARR: rajaba@mcmaster.ca

ABSTRACT:

Rapid, sensitive and selective H_2O_2 & dopamine sensors provide enormous opportunities to health, food and environmental monitoring which could prevent major social and economic devastations. To overcome the sluggish and low sensitivity of the conventional colorimetric assay, an integration of electrochemical settings with conventional assay has been proposed in this work. At first, microwave assisted cobalt MOF (Co-MOF) was synthesized using bio-linker and characterized with FESEM and TEM. The electrochemical performance of Co-MOF was examined through cyclic voltammetry (CV) where eight-fold higher currents were achieved from the Co-MOF compared to the unmodified electrode. However, Co-MOF exhibit very weak nanozymatic activity in a mixture of 3,3′,5,5′-tetramethylbenzidine (TMB) and H_2O_2. Integration of the superior electrochemical nature of Co-MOF with the nanozymatic activity resulted in a six-fold enhanced nanozymatic activity that enabled H_2O_2 quantification with a limit of detection (LOD) of 32 nM under optimized conditions. The modified electrode was further extended to quantify dopamine with a LOD of 0.81 μM where a remarkably shorter detection time (60 times shorter) has been achieved compared to the conventional nanozyme. Mechanistic study showed that the Co-MOF

View Article Online
DOI: 10.1039/D6AY00361C

provides a large surface area and abundant redox-active sites, facilitating fast electron transfer and significantly enhancing the electrochemical signal.

Keywords: Co-MOF; H_2O_2; dopamine; nanozyme; electrochemical sensor

INTRODUCTION

Metal-organic frameworks (MOFs) are crystalline and porous polymers assembled by metal ions and organic linkers. They have many unique properties including high porosity, large surface area, excellent thermal and chemical stability, mutable chemical components, and many active sites. These qualities have made them a hybrid material of interest in many areas such as chemical sensing, gas and energy storage, separation, catalysis, luminescence, and drug delivery.[1-7] Though several research articles have been reported on nanozymatic activity of MOF, most of them have discussed the specific type of MOF that showing nanozymatic activity. No one have reported the current challenges of weak nanozymatic activity of MOF, the possible way to improve the properties ands its future perspectives.

Nanozymes have shown tremendous growth in recent years due to their capability in carrying out catalytic reactions of natural enzymes while overcoming the drawbacks of natural enzymes, for example, low stability issue at different temperatures, low durability, high cost, and storing conditions. Nanozymes offer an opportunity to overcome those drawbacks of natural enzymes. To date, a large number of nanomaterials with enzyme mimicking nature have been discovered. Remarkably, it has been observed that a wide range of nanomaterials simultaneously display dual- or multi-enzyme resembling activity.[8-15] In comparison to natural enzymes, nanozymes possess higher catalytic stability, are simpler to modify, and are more affordable for mass production. Their catalytic activity may be easily regulated by modifications to their size, structure, or surface. In addition to their enzyme-like activity, nanozymes demonstrate several other properties, such as fluorescence, super-paramagnetism, and absorbance that might be helpful

View Article Online
DOI: 10.1039/D6AY00361C

for multi-applications. These unique properties of nanozyme have presented a broad range of applications ranging from *in vitro* detection, *in vivo* disease monitoring, drug delivery and replacement of certain natural enzymes in living systems, and most of all in biotechnology research. [16-22]

The ability of enzyme-integrated MOF nanozymes to function as stable enzyme supports and catalyze cascade events in a single step has also made them prominent in biosensing and biocatalysis applications. A few mono- and bi-metallic MOFs have been reported to exhibit outstanding oxidase, peroxidase, catalase, and superoxide dismutase-like activities[6].

Recent reports on Co-MOF's inherent nanozyme activity has made it possible for a selective, stable, and sensitive biosensing of glucose and H_2O_2, establishing it as an effective nanozyme and enzyme support[6]. Co-MOF is also an excellent colorimetric sensing catalyst for the detection of phosphate. The nanomaterial acts as a catalytic chromogenic platform for phosphate ions (Pi), which in excess could negatively impact the body's ability to absorb minerals and result in detrimental health issues.[23] Yuwei and co-workers reported a Co-based multifunctional nanozyme with increased catalytic active sites which was applied for the detection of environmental phenolic pollutants and disease identification.[24] Further modifications and additional component materials to the nanohybrid Co-MOF elevate its functionalities. For example, the increase of electrical conductivity of Co-MOF-74-TTF nanocomposite is useful for atmospheric gas adsorption and could be used in gas sensing[7]. Junwen and co-workers has presented a bimetallic copper/cobalt-doped nanozyme (Cu-Co-NC) for the dual-mode dopamine detection.[25] However, to the best of our knowledge, no one yet has utilized the electrical conductivity of Co-MOF to enhance its nanozymatic activity for biosensing applications. Furthermore, the integration of both electrochemical and colorimetric techniques into a unified platform, offers more advantageous

View Article Online
DOI: 10.1039/D6AY00361C

than employing either method independently. This combination provides enhanced sensitivity, dependability, and portability by facilitating the cross-verification of results, thereby minimizing the occurrence of false positives and negatives typically associated with single-mode systems.

Hydrogen peroxide (H_2O_2), a reactive oxygen species, is widely present throughout the body and plays diverse roles in physiological processes, including cellular communication, which controls immunological activation, cell proliferation, and apoptosis. However, excessive amounts of H_2O_2 might be harmful to the body, resulting in cancer, inflammatory diseases, and cell damage.[26] The reactivity and low concentration of H_2O_2 in the body make reliable detection challenging.

Moreover, the concentration of dopamine in the brain is associated with various diseases. For example, the decrease of dopamine in brain produces neurons that causes Parkinson's disease, while the excess amount of dopamine is related to schizophrenia.[25] Hence, an accurate detection system of H_2O_2 and dopamine at low concentration level is important for a quick diagnosis, to examine the disease progression and estimation of therapeutic efficiency.

The present study aims to examine the electrical nature of newly synthesized Co-MOF and apply the electrical properties of Co-MOF to improve it's nanozymatic activity. The proposed nanozymatic activity enhancement strategy is much simpler than the other techniques, namely, ligand-based enhancement, hybrid nanozyme, nanomaterials size, shape or charge dependent nanozymatic activity enhancements.[11,12,16]

In this study, the electrical conductivity of Co-MOF was utilized to enhance the nanozymatic activity. In general, the nanozymatic activity of nanomaterials perform on well plate or in microtube in the presence of TMB and H_2O_2. In this study, we have performed all the nanozymatic reaction under electrochemical parameters to achieve higher sensitivity and shorter detection time. We have introduced a new synthesis route of Co-MOF using 2,5-furandicarboxylic

View Article Online
DOI: 10.1039/D6AY00361C

acid, a bio-based linker (Scheme 1). Subsequently, we utilized the as-synthesized Co-MOF for the detection of H_2O_2 and dopamine through its electro-nanozymatic activity.

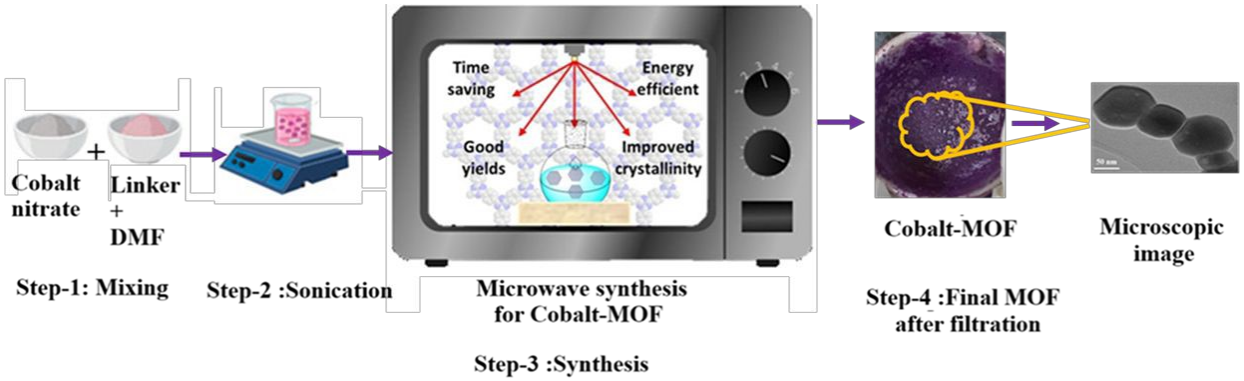

Scheme 1: The procedure of micro-wave assisted synthesis of Co-MOF.

View Article Online
DOI: 10.1039/D6AY00361C

Materials and Methods

Materials

Hydrogen Peroxide (H_2O_2), sodium acetate, cobalt nitrate hexahydrate, 2,5-furandicarboxylic acid, 3,3',5,5'-tetramethylbenzidine (TMB), tablet of phosphate buffered saline (PBS), dopamine hydrochloride, dimethylformamide (DMF) and dimethyl sulfoxide (DMSO), and ethanol were obtained from Sigma-Aldrich (Canada).

Synthesis of cobalt MOF:

Co-MOF was synthesized through a microwave-assisted method by following a previous report[1], with a slight modification in the synthesis procedure. Firstly, 0.4366 g of cobalt nitrate hexahydrate $Co(NO_3)_2.H_2O$ as the initial material, 0.3634 g of 2,5-furandicarboxylic acid as the linker and 40 mL of DMF were mixed in a beaker and stirred for 20 min to produce a homogeneous dispersion. Then the dispersion was irradiated in a microwave at 200°C, 600 W for 45 min to obtain the solid precipitate. A deep purple coloured precipitate was obtained which was washed through suction filtration with ethanol to remove the impurities. The product was dried at 60 °C in a microwave oven to obtain the Co-MOF powder.

Optimization of Co-MOF Concentration

The optimization of Co-MOF concentration was performed at the range of 0 to 70 µg/mL while TMB and H_2O_2 concentrations were kept unchanged. The concentration of Co-MOF which gave the highest absorbance represents the best concentration in this study.

TMB Optimization

The optimization of the concentration of TMB involved the preparation of different concentrations of TMB solution and its examination at a fixed concentration of H_2O_2, reaction

View Article Online
DOI: 10.1039/D6AY00361C

time, and Co-MOF concentration. Here, the concentration range of TMB was 1-8 mM with an interval of I mM. The concentration of H_2O_2 and Co-MOF was 10 µM and 70 µg/mL, respectively. The reaction was performed at room temperature for 30 min.

Optimization of pH and Reaction Time

The optimization of pH was examined in sodium acetate buffer (pH 5.2) and PBS buffer (pH 7.4), while keeping the concentration of TMB, H_2O_2 and Co-MOF constant throughout the experiment.

The reaction time was also monitored carefully by data collection for 40 seconds with a 5-seconds time interval. The time required for the concentrated blue solution to achieve the maximum absorbance peak represents the optimum reaction time.

H_2O_2 Detection

Upon completion of all the optimization steps, the detection of H_2O_2 was performed through the proposed detection method as well as conventional method. For the conventional assay, 0.1 mL of Co-MOF (40 µM) solution was added into the TMB solution (1 mL, 6 mM) in a microplate. Then, 50 µL of different concentrations (1-10 µM) of H_2O_2 was added separately. After 30 min of the reaction, the absorbance of the blue color solution of each well was recorded and a calibration curve of absorbance vs concentration of H_2O_2 was constructed.

To conduct the cyclic voltammetry (CV) analysis on a Glassy carbon electrode (GCE) was used to investigate the electro-nanozymatic process for the detection of H_2O_2, at a range of -1 V to 1 V with a scan rate of 0.1 V/s. A UV-visible spectrometer (BioTeek) was used to record the absorbance of the solution upon the appearance of a blue color within 30 seconds.

View Article Online
DOI: 10.1039/D6AY00361C

Dopamine Detection

At first, Co-MOF, TMB, H_2O_2, and 5 µL of different concentrated solution of dopamine hydrochloride solution (2-12 µM) was added separately to quantify dopamine. A UV-visible spectrometer was used to record the absorbance of the solution upon turning blue within 30 seconds.

Kinetic Assessment of TMB and H_2O_2

The kinetic parameters of Co-MOF were assessed by altering the concentration of TMB and H_2O_2. The concentration range of TMB was 0-10 mM while the concentration of H_2O_2 was fixed at 10 µM. The concentration of H_2O_2 was selected within a range of 0-10 µM while the concentration of TMB was maintained constant at 10 mM. The results were then transformed into initial velocities based on our recent article.[27] Then, the Michaelis−Menten constant (K_m) and the maximum reaction rate (V_{max}) was calculated from the Michaelis-Menten and Lineweaver-Burk plots.

Electrochemical Measurements.

A PalmSens4 potentiostat (EmStat-MUX8-R2) multiplexer was in the electrochemical measurements while a Zensor glassy carbon electrode (GCE) was the electrode and PBS at pH 7 as the electrolyte. For electrochemical measurements, 2 mg of Co-MOF was first dispersed in 2 mL of ethanol and sonicated for 15 minutes to obtain a uniform suspension. Subsequently, 5 µL of the suspension was drop-cast onto a bare glassy carbon electrode (GCE) and allowed to dry at room temperature. After drying, the modified GCE was used for electrochemical analysis.

RESULTS & DISCUSSIONS

The morphological appearance of Co-MOF was characterized by FESEM, TEM and EDX. As shown in Figure 1A (FESEM image), Co-MOF appears as a granular pearl-shape distributed

View Article Online
DOI: 10.1039/D6AY00361C

evenly on the surface. The TEM image (Fig. 1B) reveals that the synthesized Co-MOF consists of quasi-spherical particles that are closely aggregated, forming interconnected structures. The particle size is in the nanometer range, indicating successful nanoscale formation. High-resolution TEM (Fig. 1C) clearly shows lattice fringes with d-spacings of 1.34 nm, 1.21 nm, and 1.15 nm, which can be indexed to the (200), (001), and (201) crystallographic planes, respectively. These well-defined lattice fringes confirm the crystalline nature of the material at the nanoscale.

The SAED pattern (Fig. 1D) displays a series of concentric diffraction rings, indicating that the material is polycrystalline in nature with randomly oriented nanocrystallites. The appearance of rings rather than discrete spots suggests the presence of multiple crystalline domains contributing to the diffraction. The ring positions are consistent with the (200), (001), and (201) planes, which correlate well with the XRD results, confirming structural agreement between nanoscale and bulk characterization.

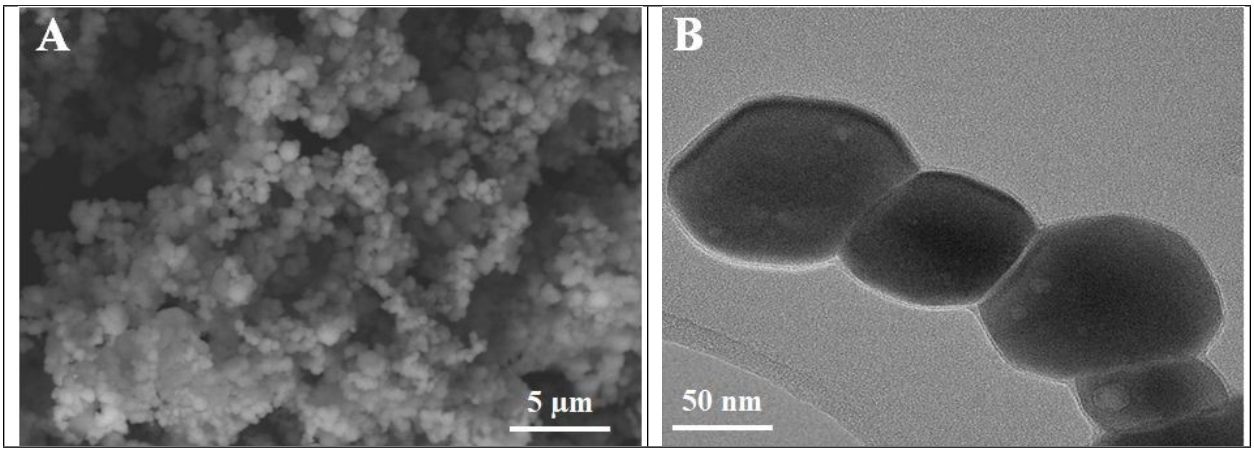

View Article Online
DOI: 10.1039/D6AY00361C

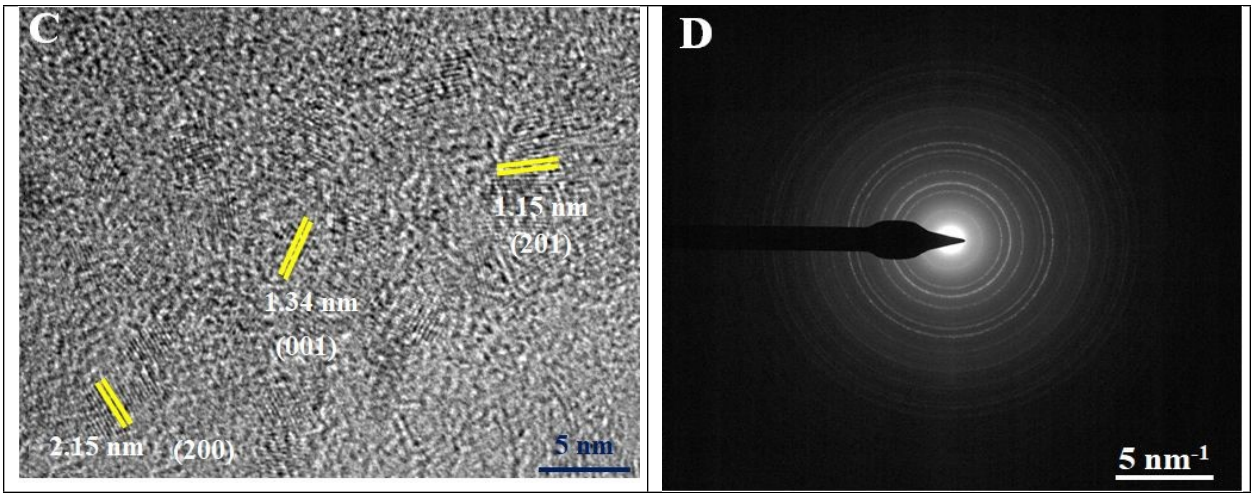

Figure 1: FESEM analysis for Co-MOF nanoparticles(A), TEM analysis for Co-MOF nanoparticles(B), Lattice space for Co-MOF nanoparticles(C) and SEAD pattern for Co-MOF nanoparticles(D).

EDX analysis (from FESEM) shows the percentage of major elements C, O, N and Co as 40.61%, 51%, 8.39%, respectively, indicating all of the main elements are present in the Co-MOF (Fig. S1).

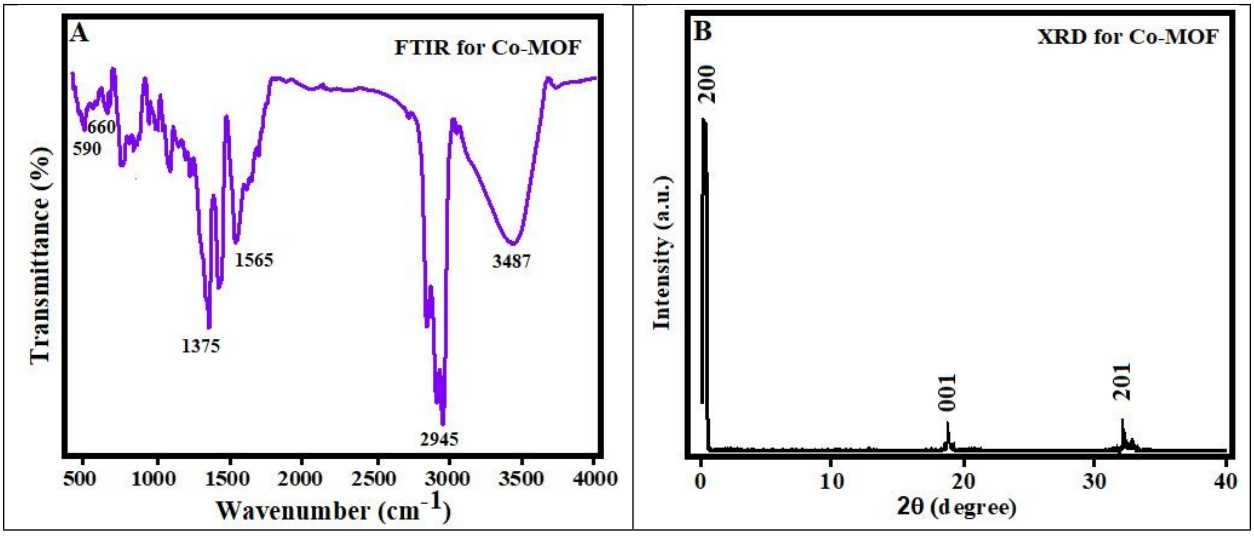

Figure 2: FTIR spectra for Co-MOF nanoparticles (A), XRD analysis for Co-MOF nanoparticles(B)

View Article Online
DOI: 10.1039/D6AY00361C

The FTIR spectrum of the synthesized material exhibits several characteristic bands confirming the formation of the Co-based framework. The absorption bands at ~590 cm^{-1} and 660 cm^{-1} are assigned to Co–O stretching vibrations, indicating the coordination between cobalt ions and the oxygen atoms of the carboxylate groups of 2,5-furandicarboxylic acid. These bands fall within the typical range reported for metal–carboxylate vibrations in Co-based metal–organic frameworks (500–700 cm^{-1}). [28,29]

For comparison, a Co–N vibration at ~442 cm^{-1} has been reported in previous study[30] which is associated with cobalt coordinated to nitrogen-containing ligands. However, such a feature is not observed in the present study. This is expected because the current system does not involve nitrogen donors; instead, cobalt coordination occurs predominantly through oxygen atoms of the carboxylate groups. In addition, the FTIR spectrum recorded in this work does not extend below 500 cm^{-1}, where the Co–N vibration is typically detected.

Furthermore, the peaks at 1565 cm^{-1} and 1375 cm^{-1} correspond to the asymmetric and symmetric stretching vibrations of the coordinated carboxylate ($–COO^-$) groups, confirming ligand–metal interaction. The band at 2945 cm^{-1} is attributed to C–H stretching vibrations, while the broad peak at 3487 cm^{-1} is assigned to O–H stretching, likely arising from adsorbed moisture or residual hydroxyl groups. These observations collectively support the successful formation of the Co–carboxylate framework.[31]

The XRD pattern of the synthesized Co-MOF (Fig. 2B) shows distinct diffraction peaks, confirming its crystalline nature. The characteristic peaks observed at 2.5°, 19.4°, and 32.5° can be indexed to the (200), (001), and (201) planes, respectively. These diffraction peaks are in good agreement with the standard JCPDS data (No. 15-0806), confirming phase purity and successful framework formation.[32]

View Article Online
DOI: 10.1039/D6AY00361C

Notably, these crystallographic planes are consistent with the lattice spacings obtained from HRTEM and the ring patterns observed in SAED, demonstrating strong agreement between bulk (XRD) and local (TEM/SAED) structural analyses.

Cyclic voltammetry (CV) was conducted to observe the electrochemical characteristics of a bare glassy carbon electrode (GCE) and a Co-MOF/GCE. As depicted in Fig. 3A at 0.5 V s^{-1} at pH 7, the unmodified GCE demonstrates a low current response with a low current response of 3 μA, indicative of slow interfacial charge transfer kinetics. In contrast, the Co-MOF/GCE exhibits a significantly maximum current response within the measured range of 25 μA, suggesting a strong interaction between the expanded surface area of Co-MOF and the ionic species present in the buffer solution. The current response of the Co-MOF/GCE is approximately eight-folds higher compared to the unmodified GCE. This increased surface area enhances charge transfer efficiency and a higher electrical conductivity thereby leading to significant electrochemical performance of the Co-MOF/GCE electrode in comparison to the unmodified GCE.

Linear sweep voltammetry (LSV) of GCE and Co-MOF/GCE is presented in Fig. 3B at 0.5 V s^{-1} with 0.5mM KOH. The unmodified GCE (curve a) exhibits a very low current response at curve a (~2 μA), whereas the Co-MOF/GCE shows a significantly enhanced current at curve b (~71.4 μA) at approximately 0.2–0.3 V potential range. This pronounced increase in current is attributed to improved electron transfer kinetics and the higher electroactive surface area of the Co-MOF-modified electrode, rather than the oxygen evolution reaction (OER), which typically occurs at much higher potentials.

Electrochemical impedance spectroscopy (EIS) was performed in 1.0 mM thiourea containing 0.1 M phosphate-buffered saline (PBS) with an amplitude of 10 mV over a frequency range of 10^{-2} to 10^{5} Hz **(Fig. 3C).** The Nyquist plots exhibit a semicircular feature in the high-frequency region,

View Article Online
DOI: 10.1039/D6AY00361C

corresponding to the charge transfer resistance (R_{ct}), while no well-defined linear Warburg diffusion region is observed at low frequencies. This indicates that the electrochemical process is predominantly controlled by charge transfer rather than diffusion. The extracted R_{ct} values are 598.36 Ω for bare GCE and 121.47 Ω for Co-MOF/GCE, confirming significantly enhanced electron transfer kinetics at the modified electrode. The smaller semicircle diameter for Co-MOF/GCE reflects its higher electrical conductivity and improved electroactive surface properties. The impedance data were fitted using an equivalent circuit consisting of solution resistance (Rs), charge transfer resistance (R_{ct}), and double layer capacitance (C_{dl}), which shows good agreement with the experimental data. These results are consistent with the CV and LSV analyses, further confirming the improved electrochemical performance of the Co-MOF-modified electrode.

Figure 3D represents the cyclic stability of the Co-MOF/GCE at 0-1.3 Volt potential range at 0.5 V s^{-1}, showing that the oxidation peak currents follow a similar pattern and exhibit no significant deviation even after 25 cycles. Therefore, Co-MOF/GCE demonstrates improved stability.

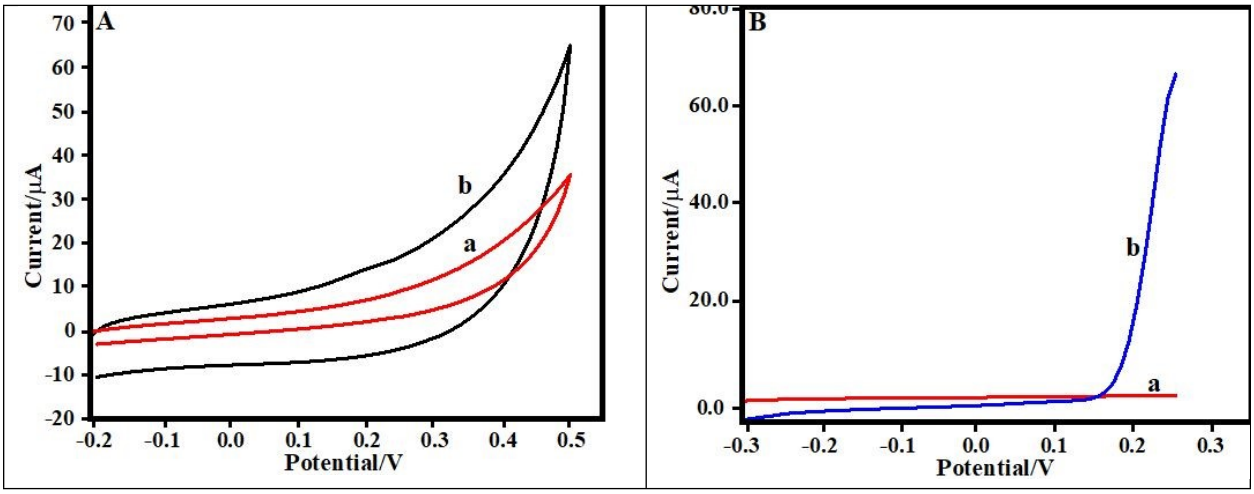

View Article Online
DOI: 10.1039/D6AY00361C

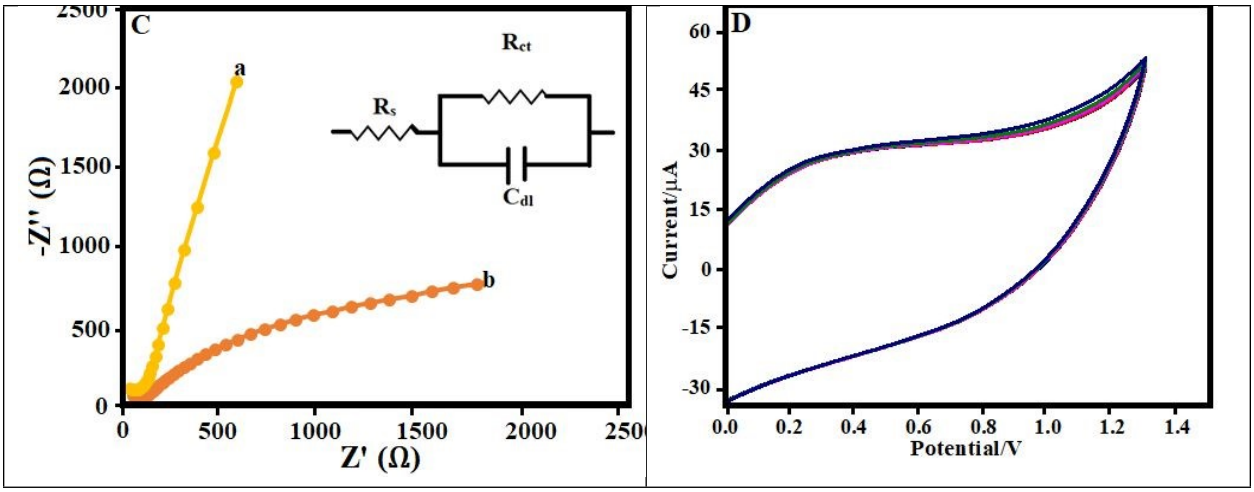

Figure 3: CV analysis for Co-MOF nanoparticles at 0.5 V s^{-1} at pH 7 (A), LSV for Co-MOF nanoparticles at 0.5 V s^{-1} with 0.5mM KOH(B), EIS analysis for the Nyquist plot of Co-MOF nanoparticles (C) and CV of Co-MOF nanoparticles at 0.5 V s^{-1} at pH 7(D).

The electrochemical analysis (CV, LSV, EIS) revealed that as-synthesized Co-MOF contains redox-active Co^{2+}/Co^{3+} centers, which facilitate rapid electron transfer and enhance electrochemical response. Unlike redox-inactive MOFs (e.g., Zn-MOF), as-prepared Co-MOF exhibits superior charge transfer kinetics due to its partially filled d-orbitals.[33] The outstanding electrochemical behavior of Co-MOF/GCE was further utilized in nanozymatic biosensing application. For example, the nanozymatic activity of Co-MOF was performed under electrochemical conditions instead of conventional microplate or microtube-based system. It is expected that the nanozymatic activity will be enhanced under the electrochemical settings (Fig 4A).

View Article Online
DOI: 10.1039/D6AY00361C

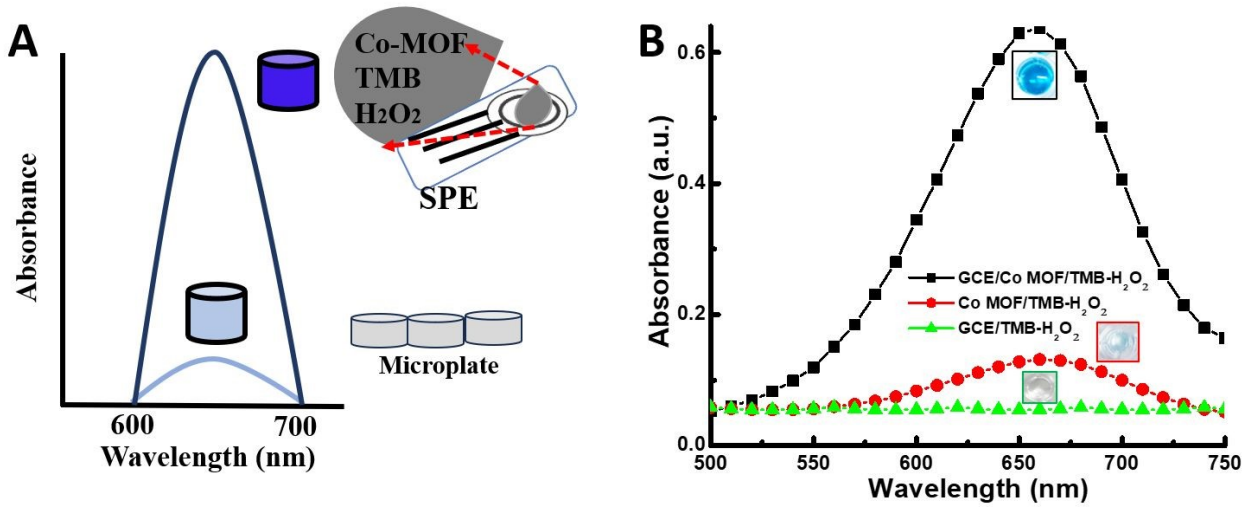

Figure 4: Schematic presentation of the modified nanozymatic activity (A) & experimental results of the proposed nanozymatic activity (B).

The feasibility of the present experimental design is presented in Figure 4B. A six-fold enhanced nanozymatic activity was observed under electrochemical setting compared to the conventional assay. No noticeable nanozymatic peak in the absence of Co-MOF was observed, indicating the significance of Co-MOF in the nanozymatic reaction. Moreover, a significant decrease in the detection time (30 minutes to 30 seconds) indicates that the proposed detection strategy offers a better sensitivity with shorter time.

View Article Online
DOI: 10.1039/D6AY00361C

As shown in Figure 5A, the nanozymatic activity is enhanced in sodium acetate buffer (pH 5.6) compared to the PBS buffer (pH 7.5). The optimized reaction time is 30 seconds (Fig 5B). The best concentration of TMB and Co-MOF in this study is 6 mM and 40 μg/mL, respectively (Fig. 5 C & D)

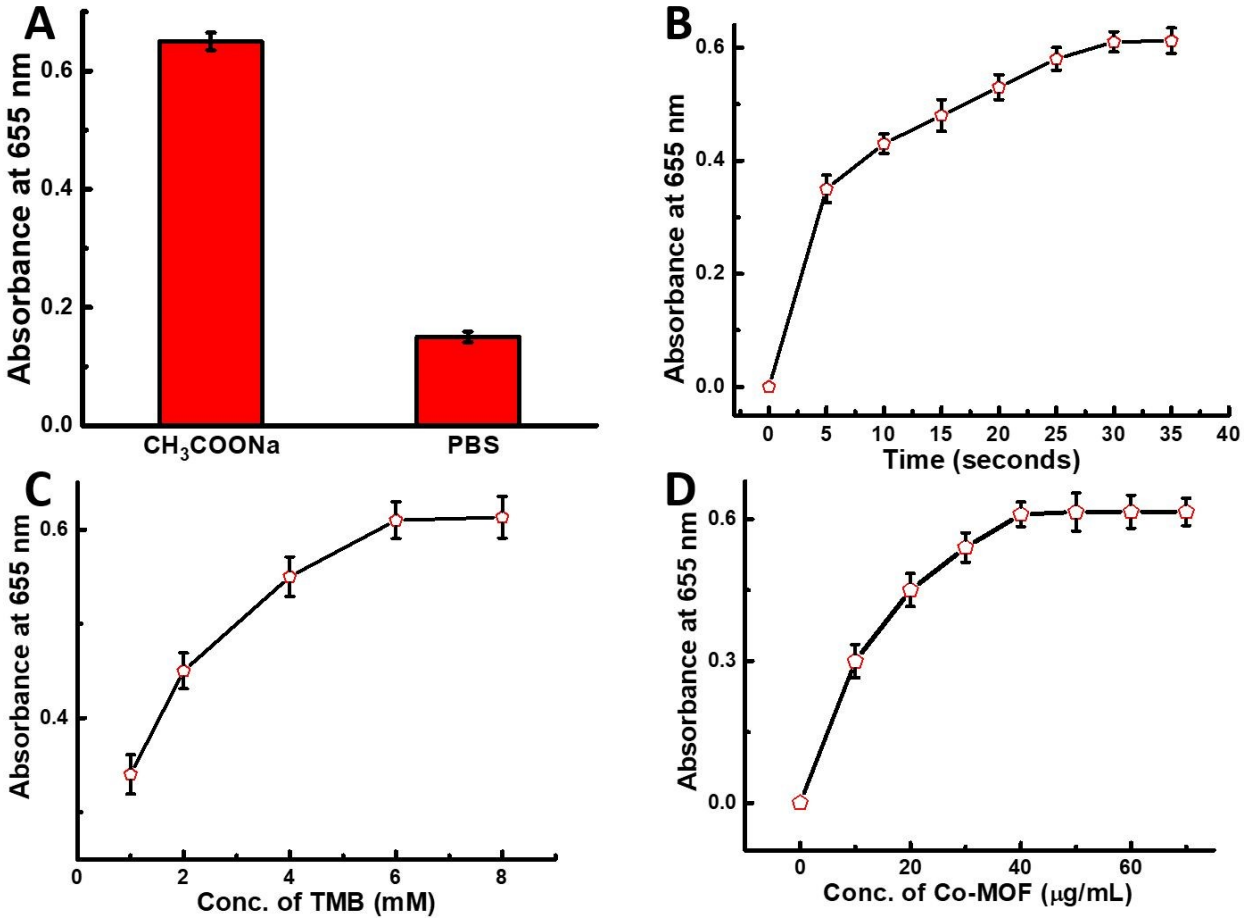

Figure 5: Optimization of (A) buffer solution; (B) reaction time; (C) concentration of TMB & (D) concentration of Co-MOF.

The sensitivity of the present assay was compared with the conventional method for the detection of H_2O_2 in buffer solution. As shown in Figure 6A, the detection range of H_2O_2 using conventional method is 1-10 μM. However, a significant lower detection range of H_2O_2 (0.1-1 μM) is achieved under electrochemical settings, indicating the superiority and novelty of the current protocol (Fig.

View Article Online
DOI: 10.1039/D6AY00361C

6B). The calculated LOD is 32 nM. The proposed H_2O_2 sensing results is comparable with the recent articles and is summarized in Table 1.

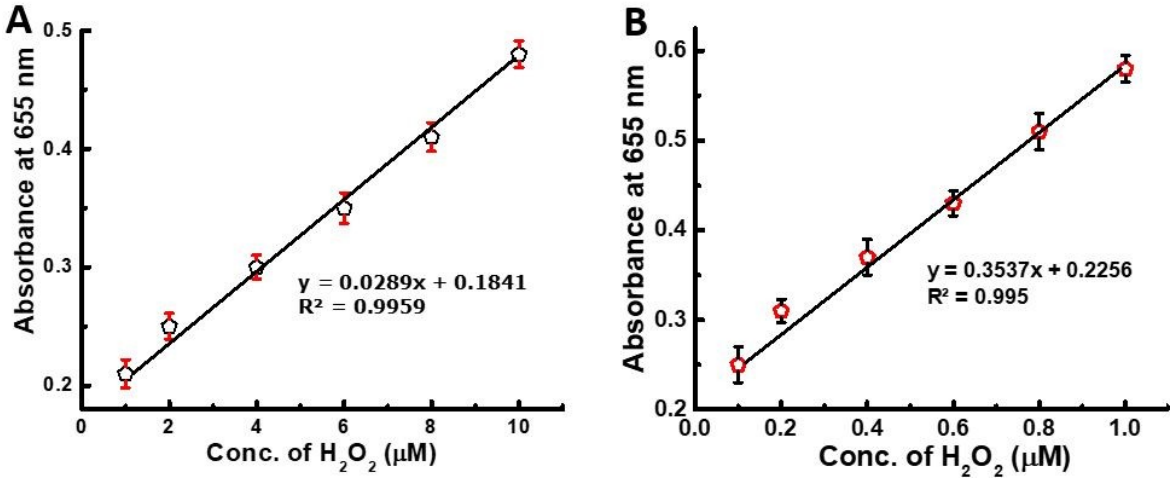

Figure 6: Detection of H_2O_2 under conventional (A) and proposed method (B).

Table 1: Comparison study of LOD values for present work with others reported for H2O2 detection.

		H_2O_2		
Nanomaterial	**Method**	**Linear Range (mM)**	**LOD (mM)**	**Ref**
Cur-AuNPs	Colorimetric	0.05 – 0.5	0.05	[34]
Fe Single-Atom	Colorimetric	0.003 – 1	0.0013	[35]
Lys-Fe-NPs	Colorimetric	0.001 – 0.2	0.00051	[36]
MB–peptide	Colorimetric	0.00002- 0.0002	0.000018	[37]
Co-MOF	Colorimetric	0.1 – 1	0.000032	Present Study

The proposed assay was further extended for the dopamine detection. As shown in Figure 7A, an inverse relationship of dopamine concentration with the absorbance of nanozymatic activity was observed due to the inhibition of dopamine. The suppression of the TMB oxidation was attributed to the depletion of hydroxyl radicals in the reaction with dopamine, thus reducing the number of available hydroxyl radicals in the reaction mixture for the oxidation of TMB molecule.[38]

View Article Online
DOI: 10.1039/D6AY00361C

The detection range of dopamine using the present method is 2-12 μM and the calculated LOD is 0.81 μM. Moreover, dopamine detection is highly specific since a very low absorbance was obtained for dopamine (12 μM) compared to other common interferent molecules with 10 times higher concentration of dopamine (120 μM) (Fig. 7B). Though norepinephrine and dopamine are structurally similar, most probably, the positive charge of dopamine strongly scavenge the negatively charged hydroxyl radial and significantly lowered the optical density.

Table 2: Comparison study of LOD values for present work with others reported for Dopamine detection.

		Dopamine		
Nanomaterial	**Method**	**Linear Range (mM)**	**LOD (mM)**	**Ref**
BSA-Cu NPs	Colorimetric	0.001 – 0.03	0.000095	[39]
Pt@N	Colorimetric	0.001 – 0.1	0.000123	[40]
Fe_3O_4@C@AgNPs	Colorimetric	0.0005 – 0.08	0.00012	[41]
$CoFe_2O_4$	Colorimetric	0.05 – 0.8	0.01	[42]
GDY QDs	Colorimetric	0.02 – 0.1	0.00865	[43]
Co-MOF	Colorimetric	0.002 - 0.012	0.00081	Present Study

The sensitivity of the proposed electro-nanozymatic dopamine detection was comparable with the recent articles, as summarized in Table 3. Most importantly, this assay could reduce the detection time significantly (from 30 min to 30 seconds).

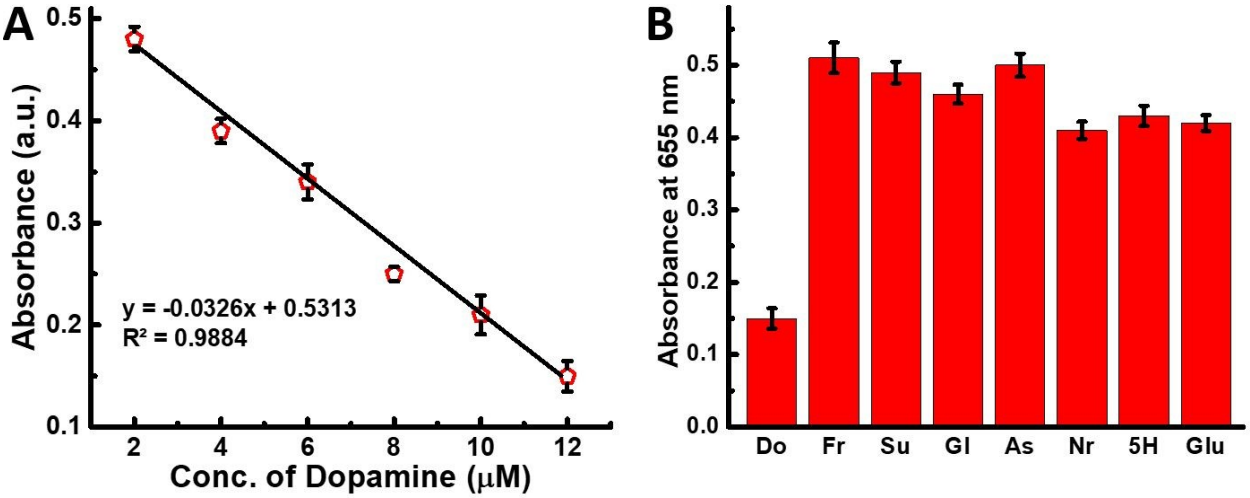

Figure 7: Detection (A) & specificity (B) of dopamine using the proposed method (Do-Dopamine,

View Article Online
DOI: 10.1039/D6AY00361C

Fr-Fructose, Su-Sucrose, Gl-Glucose, As-Ascorbic acid, Nr- Norepinephrine, 5H-5-hydroxytryptamine, Glu- glutathione).

Figure 8 presents a cyclic voltammetry (CV) plot used to investigate the electrocatalytic activity of different combinations involving hydrogen peroxide (H_2O_2), 3,3',5,5'-Tetramethylbenzidine (TMB), and a cobalt-based metal-organic framework (Co-MOF). The black curve, representing H_2O_2 alone, shows a low current response, indicating poor electron transfer process. The red curve of TMB alone exhibits a flat line with no significant redox peaks, confirming that TMB has negligible electrochemical activity under these conditions. Upon combining H_2O_2 with TMB (blue curve), the current increases moderately with the appearance of redox peaks, suggesting oxidation of TMB by H_2O_2 but with limited reaction kinetics. Notably, the pink curve, which represents the combination of H_2O_2, TMB, and Co-MOF, shows a sharp rise in the current, reaching approximately 600 μA at higher potentials, demonstrating a highly enhanced redox process and maximum electrocatalytic activity. In the final composite (pink curve), Co-MOF acts as a nanozyme via the catalytic decomposition of H_2O_2 into reactive oxygen species, which rapidly oxidizes the TMB. Additionally, Co-MOF provides a large surface area and abundant redox-active sites, facilitating fast electron transfer and significantly enhancing the electrochemical signal. This makes the Co-MOF-based composite an effective catalyst for H_2O_2 detection and TMB oxidation.

View Article Online
DOI: 10.1039/D6AY00361C

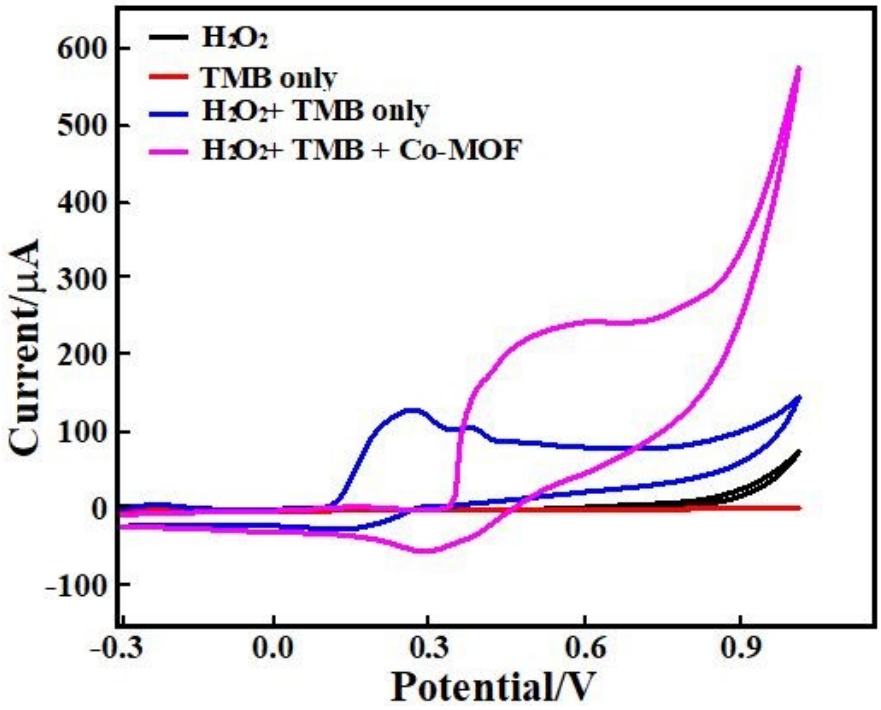

Figure 8: CVs recorded in different composite in a pH 7 PBS (0.01 M) at a scan rate of 0.5 V s^{-1} (vs. Ag/AgCl RE) on bare H_2O_2 (black curve), TMB only (red curve), H_2O_2 + TMB (blue curve) and H_2O_2 + TMB + Co-MOF electrodes.

A comparison of kinetic parameters is presented in the supporting document (Table S1) that reveals that the Co-MOF has relatively lower *K*m values indicating that it has a greater affinity for TMB and H_2O_2. As-synthesized Co-MOF has the redox-active Co^{2+}/Co^{3+} centers and partially filled d-orbitals that facilitates rapid electron transfer and exhibits superior charge transfer kinetics under the applied electrochemical force. In addition, the porous structure and high surface area of the synthesized Co-MOF provide abundant active sites and improved mass transport that significantly amplifies its catalytic performance. Moreover, the observed smaller *V*max values for Co-MOF denote that the reaction rate was slower upon saturation with its substrate.

View Article Online
DOI: 10.1039/D6AY00361C

The analytical performance of the proposed dopamine assay was further examined in simulated blood serum sample (BZ278, Biochemazone, Edmonton, Canada). The results are presented in Table 3 and reveals that the recovery percentage is in the range of 97.09-101.66 with a RSD value less than 5%. These findings strongly support the practical applicability of the proposed assay.

Table 3: Study of analytical performance of the proposed assay ion serum media

Labelled (μM)	Observed (μM)	Recovery (%)	RSD (%)
3	3.05	101.66	3.18
5	4.98	99.6	4.10
7	7.10	101.42	3.57
9	9.05	100.55	2.98
11	10.68	97.09	4.27

CONCLUSIONS

In this study, the electrochemical properties of Co-MOF were utilized to enhance its weak nanozymatic activity. At first, the environment-friendly Co-MOF was synthesized using the micro-wave method and characterized using FESEM, TEM and EDX. The as-synthesized Co-MOF has a granular pearl shape and exhibited higher electrochemical performance. The integration of electrochemically active Co-MOF with the nanozymatic activity produced a significant enhanced nanozymatic activity which was utilized for the detection of H_2O_2 and dopamine. The calculated LOD for H_2O_2 and dopamine is 32 nM and 0.81 μM, respectively. Impressively, the detection time was reduced from 30 min to 30 seconds that could be helpful to monitor a large amount of analyte with significantly shorter time. The present green synthesis of Co MOF, its integration with electrochemical setting to improve the nanozymatic activity and shorter bioanalytical detection time will promote their applications in multidisciplinary areas.

Declaration of competing interest

The authors declare that they have no known competing financial interests or personal relationships that could have appeared to influence the work reported in this paper.

Data availability

View Article Online
DOI: 10.1039/D6AY00361C

All data supporting the findings of this study are available within the article. Additional raw data can be provided by the corresponding author upon reasonable request.

Acknowledgments

The authors would like to acknowledge the support from the Natural Sciences and Engineering Research Council of Canada in the form of Discovery Grants to ARR and SS (RGPIN-2019-07246 and RGPIN-2022-04988). Also, this work was financially supported by the Ministry of Higher Education, Malaysia, for niche area research under the Higher Institution Centre of Excellence (HICoE) program (JPT(BKPI)1000/016/018/28 Jld.3(2) & NANOCAT-2024B).

Appendix A. Supplementary data

The following are the Supplementary data to this article: XXX

REFERENCES

1. A. Portorreal-Bottier, S. Gutiérrez-Tarriño, J. J. Calvente, R. Andreu, E. Roldán, P. Oña-Burgos and J. L. Olloqui-Sariego, Enzyme-like activity of cobalt-MOF nanosheets for hydrogen peroxide electrochemical sensing, *Sensors and Actuators B: Chemical*, 2022, **368, 132129.** https://doi.org/10.1016/j.snb.2022.132129

2. B. Zhu, L. Zhu, T. Hou, K. Ren, K. Kang, C. Xiao and J. Luo, Cobalt Metal–Organic Frameworks with Aggregation-Induced Emission Characteristics for Fluorometric/Colorimetric Dual Channel Detection of Nitrogen-Rich Heterocyclic Compounds, *Analytical Chemistry*, 2022, 94**(9)**, 3744–3748. https://doi.org/10.1021/acs.analchem.1c05537

3. R. M. A. Ismail, E. A. Enemose, M. Al-Jamal, S. K. Ramachandran, H. Al-Mattarneh and D. Gangodkar, Co-MoF Derived Colorimetric Sensors for Detection of Environmental Toxic Heavy Metal Analysis. *Advances in Science and Technology*, 2022, ***117,*** 43-49. https://doi.org/10.4028/p-6pqbv5

4. D. Li, S. Zhang, X. Feng, H. Yang, F. Nie and W. Zhang, A novel peroxidase mimetic Co-MOF enhanced luminol chemiluminescence and its application in glucose sensing. *Sensors and Actuators B: Chemical*, 2019, **296,** 126631–126631. https://doi.org/10.1016/j.snb.2019.126631

5. Z. Ma, Y.-S. Wang, B. Liu, H. Jiang and L. Xu, A Non–Enzymatic Electrochemical Sensor of Cu@Co–MOF Composite for Glucose Detection with High Sensitivity and Selectivity. *Chemosensors*, 2022, **10(10)**, 416. https://doi.org/10.3390/chemosensors10100416

6. B. S. Goud, G. Shin, S. P. Vattikuti, N. Mameda, H. Kim, G. Koyyada, and J. H. Kim, Enzyme-integrated biomimetic cobalt metal-organic framework nanozyme for one-step cascade glucose

View Article Online
DOI: 10.1039/D6AY00361C

biosensing via tandem catalysis. *Biochemical Engineering Journal*, 2022, **188,** 108669. https://doi.org/10.1016/j.bej.2022.108669

7 I. Strauss, A. Mundstock, M. Treger, K. Lange, S. Hwang, C. Chmelik, P. Rusch, N. C. Bigall, T. Pichler, H. Shiozawa and J. Caro, Metal–Organic Framework Co-MOF-74-Based Host–Guest Composites for Resistive Gas Sensing. *ACS Applied Materials & Interfaces*, 2019, **11(15)**, 14175–14181. https://doi.org/10.1021/acsami.8b22002

8. S. R. Ahmed, M. Sherazee, S. Srinivasan, A. R. Rajabzadeh, Positively Charged Gold Quantum Dots: An Nanozymatic "Off-On" Sensor for Thiocyanate Detection. *Foods* 2022, **11**, 1189. https://doi.org/10.3390/foods11091189.

9 S. R. Ahmed, A. G. Cardoso, S. Kumar, G. A. Ortega, S. Srinivasan, A. R. Rajabzadeh, Nanozymes in Biosensing and Bioimaging. In *Nanozymes (1st Edition)*; CRC Press, 2021.

10. S. R. Ahmed, M. Sherazee, S. Srinivasan, A. R. Rajabzadeh, Nanozymatic Detection of Thiocyanate through Accelerating the Growth of Ultra-Small Gold Nanoparticles/Graphene Quantum Dots Hybrids. *Food Chem.* 2022, **379,** 132152. https://doi.org/10.1016/j.foodchem.2022.132152.

11. S. R. Ahmed, G. A. Ortega, S. Srinivasan, A. R. Rajabzadeh, Strong Nanozymatic Activity of Thiocyanate Capped Gold Nanoparticles: An Enzyme–Nanozyme Cascade Reaction Based Dual Mode Ethanol Detection in Saliva. *New J. Chem.* 2022, **46 (3)**, 1194–1202. https://doi.org/10.1039/D1NJ03648C.

12 S. R. Ahmed, R. Chand, S. Kumar, N. Mittal, S. Srinivasan, A. R. Rajabzadeh, Recent Biosensing Advances in the Rapid Detection of Illicit Drugs. *TrAC Trends Anal. Chem.* 2020, **131**, 116006. https://doi.org/10.1016/j.trac.2020.116006.

13. M. Liang and X. Yan, Nanozymes: From New Concepts, Mechanisms, and Standards to Applications. *Accounts of Chemical Research*, 2019, **52(8)**, 2190–2200. https://doi.org/10.1021/acs.accounts.9b00140

14. X. Ren, D. Chen, Li, H. Wang, Y. Zhang, H. Chen, X. Li and M. Huo, Nanozymes-recent development and biomedical applications. *Journal of Nanobiotechnology*, 2022, **20(1)**, https://doi.org/10.1186/s12951-022-01295-y

15 S. R. Ahmed, A. G. Cardoso, H. V. Cobas, P. Das, S. Srinivasan, A. R. Rajabzadeh, Graphdiyne quantum dots for H_2O_2 and dopamine detection. *ACS Appl. Nano Mater.* 2023, **6 (10)**, 8434–8443. https://doi.org/10.1021/acsanm.3c00771.

16. S. R. Ahmed, J. Kim, T. Suzuki, J. Lee and E. Y. Park, Enhanced Catalytic Activity of Gold Nanoparticle-carbon Nanotube Hybrids for Influenza Virus Detection. *Biosens. Bioelectron.* 2016, **85**, 503−508. https://doi.org/10.1016/j.bios.2016.05.050

17. S. R. Ahmed, K. Takemeura, T. Li, N. Kitamoto, T. Tanaka, T. Suzuki, E. Y. Park, Size-Controlled Preparation of Peroxidase-like Graphene-gold Nanoparticle Hybrids for the Visible

View Article Online
DOI: 10.1039/D6AY00361C

Detection of Norovirus-like Particles. *Biosens. Bioelectron.* 2017, **87**, 558−565. https://doi.org/10.1016/j.bios.2016.08.101

18. S. R. Ahmed, J. Kim, V. T. Tran, T. Suzuki, S. Neethirajan, J. Lee and E. Y. Park, In Situ Self-assembly of Gold Nanoparticles on Hydrophilic and Hydrophobic Substrates for Influenza Virus-sensing Platform. *Sci. Rep.* 2017, **7**, 44495. DOI: 10.1038/srep44495

19. S. R. Ahmed, J. Kim, T. Suzuki, J. Lee and E. Y. Park, Detection of Influenza Virus Using Peroxidase-Mimic of Gold Nanoparticles. *Biotechnol. Bioeng.* 2016, **113**, 2298−2303. DOI: 10.1002/bit.25982

20. D. Jiang, D. Ni, Z. T. Rosenkrans, P. Huang, X. Yan and W. Cai, Nanozyme: new horizons for responsive biomedical applications. *Chemical Society Reviews*, 2019, **48(14)**, 3683–3704. https://doi.org/10.1039/C8CS00718G

21. P. Wang, D. Min, G. Chen, M. Li, L. Tong and Y. Cao, Inorganic Nanozymes: Prospects for Disease Treatments and Detection Applications. *Frontiers in Chemistry*, 2021, **9**. https://doi.org/10.3389/fchem.2021.773285

22. P. Wang, T. Wang, J. Hong, X. Yan and M. Liang, Nanozymes: A New Disease Imaging Strategy. *Frontiers in Bioengineering and Biotechnology*, 2020, **8**. https://doi.org/10.3389/fbioe.2020.00015

23. Z. Deng, H. Zhang, P. Yuan, Z. Su, Y. Bai, Z. Yin and J. He, Cobalt-Based Metal-Organic Framework Nanoparticles with Peroxidase-like Catalytic Activity for Sensitive Colorimetric Detection of Phosphate. *Catalysts*, 2022, **12(7),** 679. https://doi.org/10.3390/catal12070679

24. Yuwei Guan, Yuexiang Lu, Jingye Zhao, Wei Huang, Yueying Liu, Cobalt-based zeolitic imidazole framework incorporated with well-dispersed bimetallic nanoparticles/ions as a multifunctional nanozyme for the degradation of environmental pollutants and discrimination of various phenolic substances, Chemical Engineering Journal, 465, 2023, 142703. https://doi.org/10.1016/j.cej.2023.142703.

25. J. Feng, J. Tang, C. Jiang, C. Zhu, D. Wang, S. Tang, Bimetallic copper/cobalt-doped nanozyme based fluorescence and electrochemistry dual-modal sensor for dopamine detection ,Microchemical Journal, 222, 2026, 117147. https://doi.org/10.1016/j.microc.2026.117147

26. Li, G., Chen, Y., Liu, F. *et al.* Portable visual and electrochemical detection of hydrogen peroxide release from living cells based on dual-functional Pt-Ni hydrogels. *Microsyst Nanoeng* **9**, 152 (2023). https://doi.org/10.1038/s41378-023-00623-y

27. M. Sherazee, S. R. Ahmed, P. Das, S. Srinivasan, A. R. Rajabzadeh, Electrochemically Enhanced Peroxidase-like Activity of Nanohybrids for Rapid and Sensitive Detection of H_2O_2 and Dopamine. *Colloids Surf. Physicochem. Eng. Asp.* 2023, **679**, 132576. https://doi.org/10.1016/j.colsurfa.2023.132576.

View Article Online
DOI: 10.1039/D6AY00361C

28. Bailmare, D.B., Malozyomov, B.V. & Deshmukh, A.D. Electrodeposition of porous metal-organic frameworks for efficient charge storage. *Commun Chem* 7, 178 (2024). https://doi.org/10.1038/s42004-024-01260-w

29. Gupta, N. K., Bae, J., & Kim, K. S. (2021). Metal organic framework derived NaCoxOy for room temperature hydrogen sulfide removal. *Scientific Reports*, *11*(1), 14740.

30. Y. Xie, F. Lijiao, L. Wenbing, Z. Qin and H. Guolin, Synthesis of Mn/Co-MOF for effective removal of U (VI) from aqueous solution, *Particuology*, 2023, **72**, 134-144. https://doi.org/10.1016/j.partic.2022.03.004

31. V. T. Nam, P. T. Ni, H. N. Thu, N. N. Mai, T. A. Dung, N. T. Thanh, T. Q. Tung, T. V. Hau and T. T. Thuy, Tuning the thermal and mechanical properties of poly (vinyl alcohol) with 2, 5-furandicarboxylic acid acting as a biobased crosslinking agent." *Polymer Journal* 2022, **54**, 335-343. https://doi.org/10.1038/s41428-021-00583-y

32. X. Hu, W. Haoye, Q. Songya, S. Zilong W. Jiajun, C. Kaixuan, L. Shuji, H. Xuan, L. Shiping and X. Aijuan, Co/C nanomaterial derived from Co metal–organic framework for oxygen evolution reaction, *Ionics* 2022, **28**, 813–821. https://doi.org/10.1007/s11581-021-04376-4

33. D. M. D'Alessandro, Exploiting redox activity in metal–organic frameworks: concepts, trends and perspectives, Chem. Commun., 2016, 52, 8957. DOI: 10.1039/c6cc00805d

34. P. Sudhesh, S. Sruthi, M. Jose, K. Vyshnavi, P. Aiswarya & R. Manu, Naked eye detection of hydrogen peroxide via curcumin functionalised gold nanoparticles, Scientific Reports , 15, 2025, 16896, doi.org/10.1038/s41598-025-01613-y.

35. Y. Zhang, P. Zhao, C. Qiao, J. Zhao, Y. Liu, Z. Huang, H. Luo, C. Hou, D. Huo, Fe Single-Atom Nanozymes for Real-Time Dual Monitoring of H_2O_2 Released from Living Cells, *ACS Appl. Nano Mater.* 2023, 6, 11, 9901–9909. doi.org/10.1021/acsanm.3c01791

36. X. Hou, R. Wang, H. Zhang, M. Zhang, X. Qu, and X. Hu., Iron-Coordinated L-Lysine–Based Nanozymes with High Peroxidase-like Activity for Sensitive Hydrogen Peroxide and Glucose Detection, *Polymers* 2023, *15*(14), 3002; https://doi.org/10.3390/polym15143002

37. M. Puiu, Oana-Maria Istrate, V. Mirceski, C. Bala, Ultrasensitive Detection of Hydrogen Peroxide Using Methylene Blue Grafted on Molecular Wires as Nanozyme with Catalase-like Activity. *Anal. Chem.* 2023, 95, 44, 16185–16193. https://doi.org/10.1021/acs.analchem.3c02919

38. M. N. Ivanova**,** E. D. Grayfer**,** E. E. Plotnikova, L. S. Kibis, G. Darabdhara, P. K. Boruah, M. R. Das**,** V. E. Fedorov, *CS Appl. Mater. Interfaces* 2019, 11, 25, 22102–22112. https://doi.org/10.1021/acsami.9b04144

39. J. Xu, Z. Lv, H. Xu, Z. Mao, A sensitive dopamine colorimetric sensing platform based on Co_3ZnC/co/co-N-C nanozyme with high oxidase-like activity, Microchemical, 215, 2025, 114361, https://doi.org/10.1016/j.microc.2025.114361

View Article Online
DOI: 10.1039/D6AY00361C

40. T. Ma, X. Wang, X. Yang, Y. Mao, M. Li, Resin-Templated Synthesis of Platinum Nanozymes with Dual Oxidase and Peroxidase Activity for Dopamine Detection *ACS Appl. Nano Mater.* 2025, 8, 39, 18914–18923. doi.org/10.1021/acsanm.5c03316

41. Melisew Tadele Alula [a], Nicolette R. Hendricks-Leukes, Silver nanoparticles loaded carbon-magnetic nanocomposites: A nanozyme for colorimetric detection of dopamine, Spectrochim. Acta A Mol. Biomol. Spectrosc. 322, 2024, 124830, doi.org/10.1016/j.saa.2024.124830.

42. M. Marieeswaran, P. Panneerselvam, Self-signaling colorimetric sensor for selective detection of dopamine based on $CoFe_2O_4$ nanozyme accelerated dopamine polymerization, Analytica Chimica Acta 1338 (8), 2025, 343596. https://doi.org/10.1016/j.aca.2024.343596

43. S.R. Ahmed, et al., Graphdiyne quantum dots for H_2O_2 and dopamine detection, ACS Appl. Nano Mater. (May 2023), https://doi.org/10.1021/acsanm.3c00771.

View Article Online
DOI: 10.1039/D6AY00361C

Data availability

All data supporting the findings of this study are available within the article. Additional raw data can be provided by the corresponding author upon reasonable request.